

# Journal of Materials Chemistry A

Accepted Manuscript



This is an *Accepted Manuscript*, which has been through the Royal Society of Chemistry peer review process and has been accepted for publication.

*Accepted Manuscripts* are published online shortly after acceptance, before technical editing, formatting and proof reading. Using this free service, authors can make their results available to the community, in citable form, before we publish the edited article. We will replace this *Accepted Manuscript* with the edited and formatted *Advance Article* as soon as it is available.

You can find more information about *Accepted Manuscripts* in the [Information for Authors](#).

Please note that technical editing may introduce minor changes to the text and/or graphics, which may alter content. The journal's standard [Terms & Conditions](#) and the [Ethical guidelines](#) still apply. In no event shall the Royal Society of Chemistry be held responsible for any errors or omissions in this *Accepted Manuscript* or any consequences arising from the use of any information it contains.

# Unexplained Transport Resistances for Low-Loaded Fuel-Cell Catalyst Layers

**Adam Z. Weber\* and Ahmet Kusoglu**

Environmental Energy Technologies Division, Lawrence Berkeley National Laboratory,  
Berkeley, CA, 94720, USA

For next-generation polymer-electrolyte fuel cells, material solutions are being sought to decrease the cost of the cell components, and, in particular, the amount of catalyst, without sacrificing performance and lifetime. However, as recently shown, this cannot be achieved in practice due most likely to limitations caused by the ionomer thin-film surrounding the catalyst sites, where confinement and substrate interactions dominate and result in increased mass-transport limitations. Mitigation of this issue is paramount to the future commercial viability of polymer-electrolyte fuel cells.

To commercialize successfully polymer-electrolyte fuel cells (PEFCs), the cost must be reduced. Such cost reductions come about through simplification of balance of plant, increasing cell and stack durability and lifetime, improving cell performance, and, decreasing the cost of the cell components without sacrificing performance and lifetime. Of particular importance is this latter issue, where cell developers are trying to reduce the cost of the relatively expensive platinum-group-metal (PGM) catalysts.<sup>1</sup> As discussed below, this is a materials problem in that current architectures and materials seem to reach a bound, below which unacceptable performance losses are realized as the PGM loading is decreased. To understand the genesis of the limitations, one must understand the key processes that occur during PEFC operation. In PEFCs, the catalyst layer (CL) is a very complex chemical and geometric environment wherein the electrochemical reactions occur as shown in Figure 1a. As the figure highlights, the critical reaction for traditional PEFCs is that of oxygen reduction to water by protons (that migrate through the proton-exchange membrane) and electrons (that move through the external circuit). Due to the formation of water, the 4-electron process that is oxygen reduction, and the use of air as the oxygen carrier, the overall reaction rate is sluggish and represents the largest inefficiency of cell operation. As shown in Figure 1a, porous electrodes are used to increase electrocatalytically active surface area, where the ion-conducting polymer or ionomer binder provides proton transport pathways, the carbon particles provide electron conduction, and the void volume allows ingress and egress of gas and liquid (if present). These catalyst layers are often only 10 micrometers or so thick and their heterogeneous nature make probing their processes and structure under operation extremely challenging, thus one must rely on performance and ancillary data to derive the dominant resistances in them; new techniques to investigate transport phenomena *in operando* are needed.

Although the techniques to probe the catalyst-layer directly are sparse, combination of computational modeling and parametric cell studies have allowed for the breakdown of the various losses during operation. For the most part, this has been reliable.<sup>2</sup> However, over the past few years, stack developers began reporting on performance at low PGM loadings ( $< 0.1 \text{ mg}_{\text{PGM}}/\text{cm}^2$ ), anomalous results occurred.<sup>3-8</sup> For example, as shown in Figure 2, the undefined resistance in the cell increased with decreasing loading to substantial values,<sup>4, 7, 8</sup> and even more so at lower humidities. In this analysis, the other, known transport resistances have been removed through systematic variations in gas composition and pressure and ancillary measurements (e.g., membrane resistance by high-frequency impedance).<sup>4, 8, 9</sup> Since the unknown resistance directly impacts the ability to operate with low PGM loadings, this is a critical issue and has been gaining much attention in terms of various studies. Furthermore, such losses are seen whether one tries to decrease the loading by making the catalyst-layer thinner or by diluting the catalyst layer by carbon particles without catalyst (i.e., decreasing the Pt/C ratio but keeping overall layer thickness constant as shown in Figure 1b). Similarly, even higher loaded catalyst layers can exhibit increased resistance after undergoing degradation tests, wherein the active surface area is decreased due to different phenomena,<sup>10</sup> and whose effect is dependent on the carbon substrate as well.<sup>11</sup> For example, Jomori *et al.*<sup>12</sup> witnessed a doubling of the unexplained cathode catalyst-layer resistance after potential cycles wherein the effective catalyst surface area is decreased, consistent with other studies.<sup>13</sup> <sup>14</sup> Finally, it should be noted that for low effective PGM loadings, the crossover hydrogen through the membrane can generate more severe mixed potentials.

The unknown resistance or voltage loss scales with the Pt surface-area specific current density (as opposed to geometric-area specific current density), meaning that the resistance is related to local effects at the catalytic site, but is not related to the turnover frequency of the catalyst as one can

collapse the data on a master polarization curve normalized to the electrochemically active Pt surface area. Thus, the local resistance appears to be related to the fact that the flux per platinum site increases with decreasing loading as shown schematically in Figure 1b, thereby making it harder for oxygen to reach the active site; similarly, heat and water production will also be locally higher. This increased flux means that any resistance of oxygen to the Pt surface is exacerbated as is any poisoning or site blockage. This analysis also agrees with the above concepts of lower effective loadings after accelerated durability tests as well as the dependence of the observed catalyst-layer dependence on humidity, which is similar to that of the membrane or bulk ionomer.<sup>15</sup> Thus, the measured local resistance is assumed to be the sum of three component resistances from the gas phase to the Pt surface:<sup>8, 13</sup> the interfacial resistance at the gas/ionomer interface, the bulk resistance of the ionomer film, and the interfacial resistance at the ionomer/Pt interfaces, which is related to possible adsorption of the ionomer acid moieties onto the Pt surface (Figure 1c).<sup>16-18</sup> Quantification of each resistance would provide key knowledge, however, in practice they are very coupled and undoubtedly impact each other and so may not be separable. A notable exception is the model of Debe<sup>19</sup> that used the kinetic theory of gases to derive the probability of oxygen reaching a greatly dispersed Pt site to explain the observed increased resistance at low Pt loadings.

Various studies have shown that the unknown resistance is not able to be rationalized fully based on known ionomer thickness (on the order of 2 to 10 nanometers) and bulk ionomer transport properties (e.g., see reference <sup>20</sup>). Thus, the film and interfacial process of oxygen into it must be more resistive than the bulk. This concept is in agreement with recently observed low water content in the catalyst-layer ionomer compared to the bulk ionomer membrane.<sup>21-23</sup> With the lower water contents, one expects lower transport properties. For oxygen, this seems to be the case at least down to 100 nm or so

films,<sup>24</sup> and more data is required for thinner films. However, while some studies have shown lower proton conductivity,<sup>6, 21, 25-27</sup> others have shown increases in it.<sup>28-30</sup> This discrepancy may be due to measurement methods, anisotropic conductivity, or perhaps secondary ion-conduction pathways such as water films; more data is required to understand the critical materials properties and relate them to the structure/function relationships of the ionomer. These relationships are expected to perhaps change as the ionomer thickness decreases and confinement effects become dominant.<sup>23</sup>

It is well known that when a polymer is confined to thicknesses comparable to its characteristic domain size, its properties and morphology differ from the analogous bulk materials.<sup>31</sup> Even though confinement effects in polymer films have long been of interest, films of naturally phase-separated ionomers, such as those used in PEFCs, have gained attention only recently, especially in the last year or so.<sup>32-41</sup> Ion-containing polymers are more complex than many widely studied polymers due to the presence of solvent/ion electrostatic interactions, hydrogen bonding, less defined chain structure, and their self-assembly is expected to be affected by wetting interactions at both the substrate and free (vapor/liquid) interfaces as well as by topological confinement effects. The ionomer thin-film studies have reported confinement-driven changes in properties including water-uptake rate and value, which are assumed to serve as proxies for other transport phenomena. In general, a significant deviation from bulk behavior is observed when the films are confined to thicknesses of less than 100 nm, where there is a decrease in water content until one gets to very thin-films (< 20 nm), as shown in Figure 3, where the lack of being able to form crystallites might correlate to the observed increase in water content.<sup>34, 39</sup> The exact magnitude of these changes largely depends on the processing conditions, casting solution, and substrate. The values and trends are in agreement with those derived from catalyst-layer studies in terms of both water contents as well as time constants for water uptake, implying that the thin films can

serve as models for catalyst-layer ionomer. However, the nature of the above changes is not definitively known.

Recently, the research focus has been on correlating the observed uptake and associated swelling changes to the morphology of the thin films in order to understand the origins of the confinement-driven changes in transport properties. Recent studies have demonstrated that confinement effects and wetting interactions result in different morphological properties of the ionomer thin films as shown by various techniques including grazing-incidence small-angle X-ray Scattering (GISAXS),<sup>34, 39, 41-43</sup> reflectivity,<sup>41, 44</sup> x-ray and neutron reflectivity,<sup>41, 44, 45</sup> TEM,<sup>34</sup> fluorescence,<sup>33</sup> contact angle,<sup>40, 46</sup> and positron annihilation.<sup>47</sup> GISAXS has been shown to be extremely useful to investigate the orientation and spacing of the domains at and below the thin-film interfaces. Similar to the water-content studies, one sees a loss in phase-separation as films approach thicknesses on the order of 20 nm (see Figure 3).<sup>39</sup> The initial deviation in structure/swelling relationship from bulk behavior can be attributed to the confinement effects in thin-films (of less than 100 nm) in which the polymer and water domains cannot randomly orient themselves as in the bulk. However, with a further decrease in thickness below 20 nm, the lack of structure or phase separation is seemingly accompanied by increased swelling as the ionomer exhibits more or less a dispersion-like behavior (see Figure 3). In addition, recent studies also seem to suggest that domain orientation closer to the support could be aligned depending on the substrate material,<sup>33, 39, 44, 45</sup> and, in particular, its hydrophobicity,<sup>45, 48, 49</sup> where increased anisotropy is witnessed, which is similar to interfacial changes in bulk ionomers caused by the environment.<sup>50-59</sup> This alignment also seemingly correlates to an increase in the modulus of thin films,<sup>60</sup> which is somewhat consistent with the reduced water uptake due to a shifting balance of mechanical/chemical energies controlling the swelling. In addition, the films themselves exhibit wettability changes depending on thickness and

substrate with films changing from hydrophobic to hydrophilic in ambient conditions around 50 nm on Si,<sup>40, 47</sup> but not until much lower thicknesses on Pt,<sup>40, 47</sup> suggesting the importance of substrate interactions. Overall, the current materials understanding of ionomer thin films is still far from complete due to the significant material-parameter space (e.g., film thickness, casting and processing conditions, substrate, *etc.*) and experimental and computational difficulties, and one needs to determine the governing relationships in order to elucidate the causes of resistance in hopes of mitigating them through material design and manipulation. Furthermore, most current studies focus on planar films under *ex-situ* conditions, thus, there is need to understand fundamentally how these interactions occur on real particles with varying surface area and under operating conditions including application of electrochemical potential.

As discussed, PEFCs made with traditional Pt/C catalyst layers demonstrate unexplained resistances at low PGM loadings that seem related to the ionomer film surrounding the catalyst sites. These films interact with the sites in a variety of ways, and only by understanding the role of film thickness and substrate/film interactions in the structure-function relationships of thin-film ionomers, can one develop tools, structures, and materials to achieve optimum ionomer content, better PGM utilization, and ultimately improved catalyst-layer performance. One should also note that the above discussion could also represent a possible issue with higher-loaded catalyst layers, which may become low-loaded during operation due to degradation. There is a need to explore the steady and dynamic behavior of the morphological, structural, and transport properties of thin-films, including possible anisotropies. In addition, there is ample opportunity to look towards material solutions to decrease the ionomer-film resistance, which could be different ionomer structures, side-chains and acid endgroups, different ion-exchange capacities, more gas-permeable morphologies and backbone moieties, different casting



solvents and thermal treatments, different substrate (*i.e.*, carbon) properties, *etc.* While some challenges with low-PGM-loaded catalyst layers can perhaps be engineered around (for example, one can remove the ionomer entirely as exemplified by 3M's NSTF electrodes),<sup>61</sup> such approaches typically compromise other aspects of cost whether it is performance or durability. Similarly, while alternative, non PGM,<sup>62</sup> or more active catalysts<sup>63</sup> can be explored, the issues related to oxygen accessibility may or may not be mitigated.

## References

1. *Fuel Cell Technologies Office Multi-Year Research, Development and Demonstration Plan*, U.S. Department of Energy, 2013.
2. H. A. Gasteiger, J. E. Panels and S. G. Yan, *Journal of Power Sources*, 2004, **127**, 162-171.
3. R. Makharia, in *8th International Fuel Cell Science, Engineering & Technology Conference*, ASME, Brooklyn, NY, 2010.
4. N. Nonoyama, S. Okazaki, A. Z. Weber, Y. Ikogi and T. Yoshida, *Journal of the Electrochemical Society*, 2011, **158**, B416-B423.
5. S. Jomori, N. Nonoyama and T. Yoshida, *J. Power Sources*, 2012, **215**, 18-27.
6. A. Ohma, T. Mashio, K. Sato, H. Iden, Y. Ono, K. Sakai, K. Akizuki, S. Takaichi and K. Shinohara, *Electrochimica Acta*, 2011, **56**, 10832-10841.
7. Y. Ono, T. Mashio, S. Takaichi, A. Ohma, H. Kanesaka and K. Shinohara, *ECS Trans.*, 2010, **28 (27)**, 69-78.
8. J. P. Owejan, J. E. Owejan and W. Gu, *J. Electrochem. Soc.*, 2013, **160**, F824-F833.
9. T. A. Greszler, D. Caulk and P. Sinha, *J. Electrochem. Soc.*, 2012, **159**, F831-F840.
10. R. Borup, in *DOE Hydrogen Annual Merit Review*, Crystal City, VA, 2007.
11. R. Mukundan, G. James, D. Ayotte, J. R. Davey, D. Langlois, D. Spornjak, D. Torraco, S. Balasubramanian, A. Z. Weber, K. L. More and R. L. Borup, *ECS Transactions*, 2013, **50**, 1003-1010.
12. S. Jomori, N. Nonoyama and T. Yoshida, *Journal of Power Sources*, 2012, **215**, 18-27.
13. S. Jomori, K. Komatsubara, N. Nonoyama, M. Kato and T. Yoshida, *Journal of the Electrochemical Society*, 2013, **160**, F1067-F1073.
14. S. V. Selvaganesh, G. Selvarani, P. Sridhar, S. Pitchumani and A. K. Shukla, *Phys Chem Chem Phys*, 2011, **13**, 12623-12634.
15. H. Iden, S. Takaichi, Y. Furuya, T. Mashio, Y. Ono and A. Ohma, *J Electroanal Chem*, 2013, **694**, 37-44.
16. R. Subbaraman, D. Strmcnik, A. P. Paulikas, V. R. Stamenkovic and N. M. Markovic, *Chemphyschem*, 2010, **11**, 2825-2833.
17. R. Subbaraman, D. Strmcnik, V. Stamenkovic and N. M. Markovic, *J Phys Chem C*, 2010, **114**, 8414-8422.
18. S. Jomori, K. Komatsubara, N. Nonoyama, M. Kato and T. Yoshida, *J. Electrochem. Soc.*, 2013, **160**, F1067-F1073.
19. M. K. Debe, *Journal of the Electrochemical Society*, 2012, **159**, B54-B67.
20. W. Yoon and A. Z. Weber, *Journal of The Electrochemical Society*, 2011, **158**, B1007-B1018.
21. H. Iden, K. Sato, A. Ohma and K. Shinohara, *Journal of the Electrochemical Society*, 2011, **158**, B987-B994.
22. A. Kusoglu, A. Kwong, K. T. Clark, H. P. Gunterman and A. Z. Weber, *Journal of the Electrochemical Society*, 2012, **159**, F530-F535.
23. S. Holdcroft, *Chem Mater*, 2014, **26**, 381-393.
24. T. Suzuki, K. Kudo and Y. Morimoto, *Journal of Power Sources*, 2013, **222**, 379-389.
25. J. Peron, D. Edwards, M. Haldane, X. Y. Luo, Y. M. Zhang, S. Holdcroft and Z. Q. Shi, *Journal of Power Sources*, 2011, **196**, 179-181.
26. A. Suzuki, U. Sen, T. Hattori, R. Miura, R. Nagumo, H. Tsuboi, N. Hatakeyama, A. Endou, H. Takaba, M. C. Williams and A. Miyamoto, *Int J Hydrogen Energ*, 2011, **36**, 2221-2229.

27. T. Soboleva, K. Malek, Z. Xie, T. Navessin and S. Holdcroft, *ACS applied materials & interfaces*, 2011, **3**, 1827-1837.
28. K. C. Hess, W. K. Epting and S. Litster, *Analytical Chemistry*, 2011, **83**, 9492-9498.
29. R. Makharia, M. F. Mathias and D. R. Baker, *Journal of the Electrochemical Society*, 2005, **152**, A970-A977.
30. S. J. An and S. Litster, *ECS Transactions*, 2013, **58**, 831-839.
31. T. P. Russell, P. Lambooy, G. J. Kellogg and A. M. Mayes, *Physica B*, 1995, **213**, 22-25.
32. P. Krtil, A. Trojanek and Z. Samec, *Journal of Physical Chemistry B*, 2001, **105**, 7979-7983.
33. S. K. Dishari and M. A. Hickner, *ACS Macro Letters*, 2012, **1**, 291-295.
34. M. A. Modestino, D. K. Paul, S. Dishari, S. A. Petrina, F. I. Allen, M. A. Hickner, K. Karan, R. A. Segalman and A. Z. Weber, *Macromolecules*, 2013, **46**, 867-873.
35. P. Bertonecello, I. Ciani, F. Li and P. R. Unwin, *Langmuir*, 2006, **22**, 10380-10388.
36. Z. Siroma, R. Kakitsubo, N. Fujiwara, T. Ioroi, S. I. Yamazaki and K. Yasuda, *Journal of Power Sources*, 2009, **189**, 994-998.
37. A. Kongkanand, *The Journal of Physical Chemistry C*, 2011, **115**, 11318-11325.
38. S. K. Dishari and M. A. Hickner, *Macromolecules*, 2013, **46**, 413-421.
39. A. Kusoglu, D. Kushner, D. K. Paul, K. Karan, M. A. Hickner and A. Z. Weber, *Advanced Functional Materials*, 2014, in press.
40. D. K. Paul, K. Karan, A. Docoslis, J. B. Giorgi and J. Pearce, *Macromolecules*, 2013, **46**, 3461-3475.
41. S. A. Eastman, S. Kim, K. A. Page, B. W. Rowe, S. Kang, C. L. Soles and K. G. Yager, *Macromolecules*, 2012, **45**, 7920-7930.
42. M. A. Modestino, A. Kusoglu, A. Hexemer, A. Z. Weber and R. A. Segalman, *Macromolecules*, 2012, **45**, 4681-4688.
43. M. Bass, A. Berman, A. Singh, O. Konovalov and V. Freger, *Macromolecules*, 2011, **44**, 2893-2899.
44. J. A. Dura, V. S. Murthi, M. Hartman, S. K. Satija and C. F. Majkrzak, *Macromolecules*, 2009, **42**, 4769-4774.
45. D. L. Wood, J. Chlistunoff, J. Majewski and R. L. Borup, *J Am Chem Soc*, 2009, **131**, 18096-18104.
46. D. K. Paul and K. Karan, *J Phys Chem C*, 2014, **118**, 1828-1835.
47. H. F. M. Mohamed, S. Kuroda, Y. Kobayashi, N. Oshima, R. Suzuki and A. Ohira, *Phys Chem Chem Phys*, 2013, **15**, 1518-1525.
48. T. Mashio, K. Malek, M. Eikerling, A. Ohma, H. Kanesaka and K. Shinohara, *J Phys Chem C*, 2010, **114**, 13739-13745.
49. G. Dorenbos, V. A. Pomogaev, M. Takigawa and K. Morohoshi, *Electrochem Commun*, 2010, **12**, 125-128.
50. G. S. Hwang, D. Y. Parkinson, A. Kusoglu, A. A. MacDowell and Adam Z. Weber, *ACS Macro Letters*, 2013, **2**, 288-291.
51. A. Kusoglu, M. A. Modestino, A. Hexemer, R. A. Segalman and A. Z. Weber, *ACS Macro Letters*, 2012, **1**, 33-36.
52. Q. He, I. T. Lucas, A. Kusoglu, A. Z. Weber and R. Kostecky, *Journal of Physical Chemistry B*, 2011, **115**, 11650-11657.
53. K.-D. Kreuer, *Solid State Ionics*, 2013.
54. N. Takimoto, L. Wu, A. Ohira, Y. Takeoka and M. Rikukawa, *Polymer*, 2009, **50**, 534-540.
55. Y. Kang, O. Kwon, X. Xie and D.-M. Zhu, *Journal of Physical Chemistry B*, 2009, **113**, 15040-15046.
56. N. Takimoto, A. Ohira, Y. Takeoka and M. Rikukawa, *Chemistry Letters*, 2008, **37**, 164-165.

57. E. Aleksandrova, R. Hiesgen, K. A. Friedrich and E. Roduner, *Phys Chem Chem Phys*, 2007, **9**, 2735-2743.
58. A. M. Affoune, A. Yamada and M. Umeda, *Journal of Power Sources*, 2005, **148**, 9-17.
59. M. Bass, A. Berman, A. Singh, O. Konovalov and V. Freger, *Journal of Physical Chemistry B*, 2010, **114**, 3784-3790.
60. K. A. Page, A. Kusoglu, C. M. Stafford, S. Kim, R. J. Kline and A. Z. Weber, *Nano Letters*, 2014, **14**, 2299-2304.
61. M. K. Debe, *Nature*, 2012, **486**, 43-51.
62. G. Wu, K. L. More, C. M. Johnston and P. Zelenay, *Science*, 2011, **332**, 443-447.
63. V. R. Stamenkovic, B. S. Mun, M. Arenz, K. J. J. Mayrhofer, C. A. Lucas, G. Wang, P. N. Ross and N. M. Markovic, *Nature Materials*, 2007, **6**, 241-247.

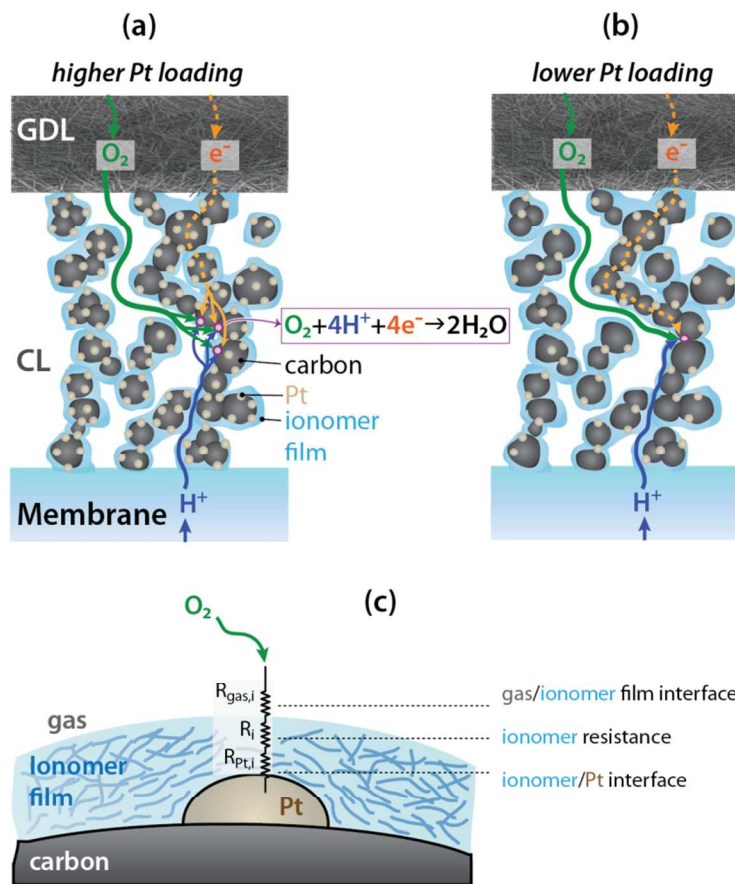


**Figure 1** Schematics of the porous fuel-cell catalyst-layer structure and the transport therein for (a) high and (b) low PGM loadings. (c) Close up view of local transport to a Pt site through the ionomer film showing the orientation of polymer domains and transport resistances.

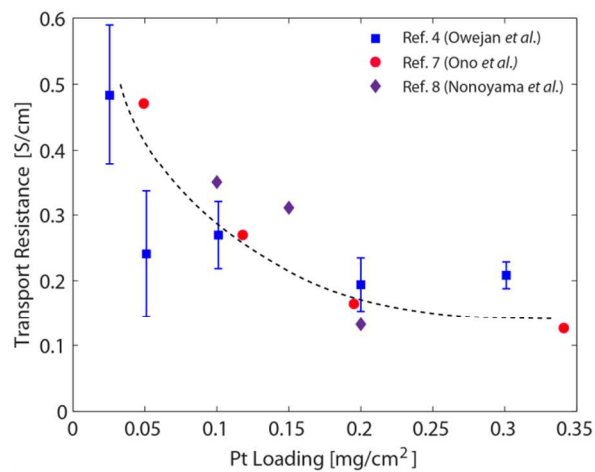


**Figure 2.** Undefined cell resistance as a function of Pt loading based on references<sup>4,7,8</sup> (dotted line is only guide for the eye) at near 100 % relative humidity, where all known resistances have been systematically corrected.

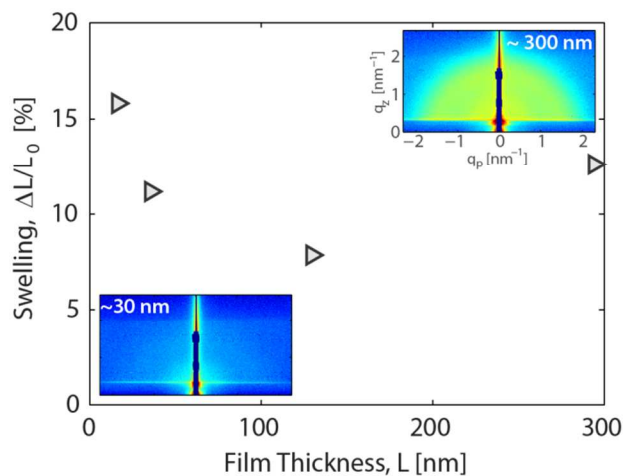
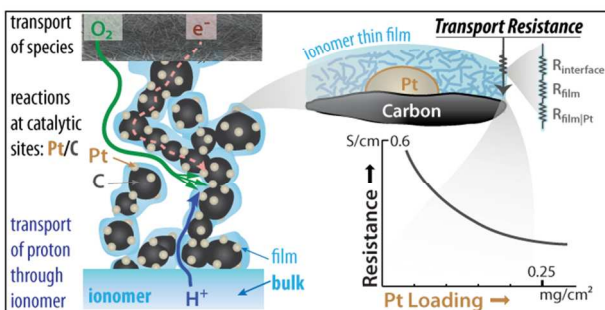


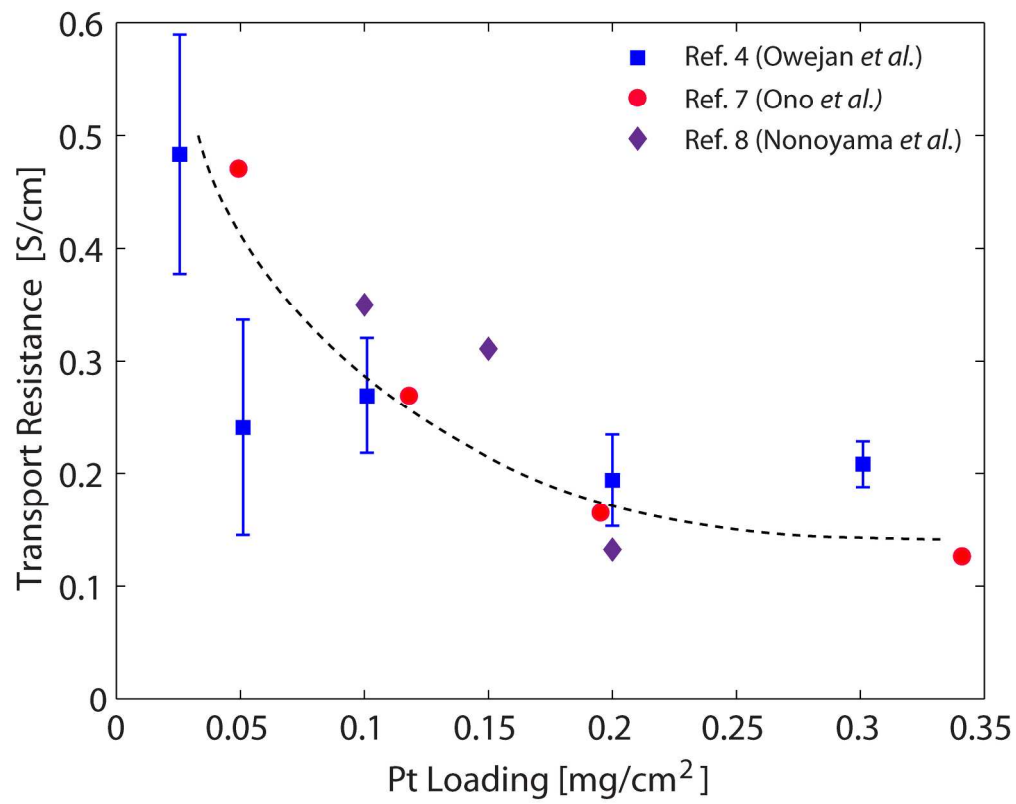
**Figure 3.** Ellipsometry and GISAXS (inset) data for Nafion thin films on carbon close to saturation (95 to 100% relative humidity).<sup>39</sup> GISAXS half-ring becomes weaker as the film gets thinner (i.e., from 300 nm to ~30 nm in the insets) indicating weaker or complete loss of phase separation. Thickness swelling of films of ~100 nm decreases due to deviation from bulk-like structure, then increases again for thicknesses close to or below 20 nm due to loss of structure.

## Table of Contents Graphic



Mass-transport limitations in fuel-cells due to the resistances caused by the ionomer thin-film surrounding the catalyst sites must be mitigated to achieve the desired performance with low-Pt loadings, a key for the commercialization of polymer-electrolyte fuel cells.





108x86mm (600 x 600 DPI)